CUMULATIVE BIREFRINGENCE EFFECTS OF NANOSECOND LASER PULSES IN DYE-DOPED PLANAR NEMATIC LIQUID CRYSTAL LAYERS

SVETLANA G. LUKISHOVA*, ROBERT W. BOYD and NICK LEPESHKIN

The Institute of Optics, University of Rochester, Rochester, NY 14627-0186, USA
*lukishov@optics.rochester.edu

KENNETH L. MARSHALL

Laboratory for Laser Energetics, University of Rochester,
250 East River Road, Rochester, NY 14623-1299, USA

New *cumulative* effects in laser-induced birefringence have been observed under 10-Hz-pulse-repetition-rate, nanosecond-duration laser irradiation of azo-dye-doped planar-nematic liquid crystal layers at incident intensities I $\sim$ 1–10 MW/cm^2. An irradiation geometry with the incident polarization *parallel* to the nematic director was used. This geometry does not permit a first-order electric field induced reorientation of the nematic molecules, allowing us to exclude its contribution to the nonlinear response. New laser-induced birefringence effects with a buildup time of several seconds to minutes manifest themselves in:

- the appearance of a polarization component *perpendicular to the nematic director*;
- two different modes of spatial pattern formation with different patterns for parallel and perpendicular polarization:
  (1) At I $\sim$ 1–5 MW/cm^2, the *perpendicular* polarization component forms a four-leaf-clover (a Maltese-like cross) spatial pattern in the far-field from the initial Gaussian spatial intensity distribution. The incident, *parallel* polarization component forms a round spot with a single ring spatial pattern.
  (2) At higher incident intensities (I $\sim$ 5–10 MW/cm^2), a second regime of pattern formation is observed in the form of high definition patterns and only for the polarization component *parallel* to the nematic director.

Keywords: Liquid crystals; pattern formation; induced birefringence.

1. Introduction

Cumulative effects connected with light absorption of pulsed laser radiation and laser-induced local heating of a material are seldom studied at a l0-Hz pulse repetition rate, a common regime in optical power limiting applications and Z-scan measurements. However, recently they were reported[1,2] in thermal-nonlinearity studies of $\sim$ 100-μm thick *liquid-crystal* (LC) layers. The present paper describes an additional manifestation of cumulative effects in heating of azo-dye-doped

planar nematic LCs by *low-repetition-rate*, nanosecond laser radiation. Thin, 10–20-μm thickness layers were used. New cumulative effects in heating reported in the present paper appear as induced-birefringence effects and spatial pattern formation. These results are useful for photonic devices based on thin layers of LCs absorbing repetitively pulsed, focused laser radiation, for instance, optical power limiters, 1-D photonic-band-gap chiral nematic LC lasers[3–6] and LC single-photon sources.[7]

The structure of this paper is as follows. Section 2 describes the experimental set up and planar-aligned LC-layer scheme used in the experiments. Section 3 describes the characterization of our materials and LC-cell fabrication. In Sec. 4 the results on polarization-dependent spatial patterns in laser beam cross-section are reported, including low-intensity patterns in the four-leaf-clover (Maltese-like cross) form (Sec. 4.1) and high-intensity patterns in the form of concentric rings for polarization parallel to the nematic director (Sec. 4.2). Section 5 presents the experimental results of Z-scan measurements of nonlinear-transmittance enhancement in azo-dye-doped LC-layer. In Sec. 6 the mechanisms producing the described phenomena for low (Sec. 6.1) and high (Sec. 6.2) incident intensities are discussed. Section 7 concludes the paper.
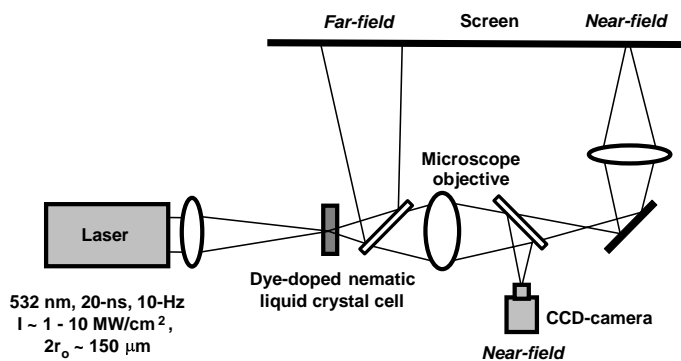
2. Experimental Set Up

The experimental set up is shown in Fig. 1(a). A 1.064-μm, passively Q-switched Nd:YAG laser, using a single-longitudinal-mode resonator and two-pass amplifier, provided at 5- or 10-Hz repetition rates a Gaussian beam spatial and temporal intensity distribution with output energy of up to 20 mJ. The 1.064-μm-beam was focused into a KTP second harmonic crystal with a 1-m-focal-length lens. After the separation of the fundamental frequency by a highly absorbing filter, the 0.532-μm laser beam with a pulse duration of $\sim$ 20–26 ns was focused by the 24-cm-focal-length lens into the dye-doped planar-aligned nematic LC cell (Fig. 1(b)). The incident polarization was parallel to the orientation of the rod-like nematic LC molecules (director). The beam diameter in the focus was $\sim$ 150 μm at the $1/e$ level.

The far-field patterns were recorded from a screen by a video camera onto magnetic tape from which intensity distribution from each pulse was digitized afterwards. The near field patterns were confined to the focal area. They were recorded either by a CCD-camera using a 4$\times$ microscope objective or by the video camera from the screen, using an additional lens for 500$\times$ magnification. For imaging the near-field and for calibration, a special cell made from identical glass substrates as the dye-doped LC cell, but with a reticle inside, was used in place of the LC cell.

3. Liquid Crystal Cell Preparation and Characterization

The nematic LC mixture E7 of mostly cyanobiphenyl compounds (Fig. 2(a)) doped with the azo-dye "Oil Red O" (Fig. 2(b)) with a 1.5% weight-concentration
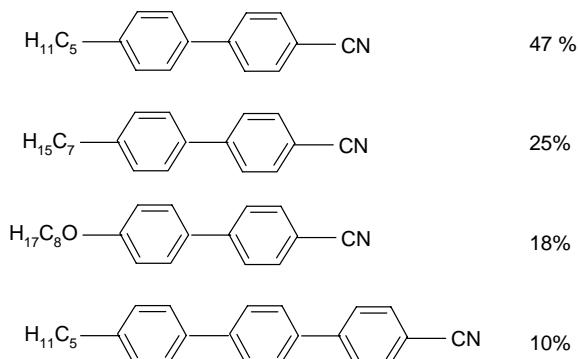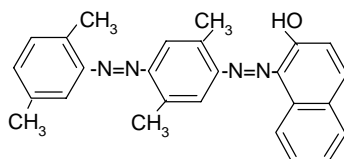
(a)
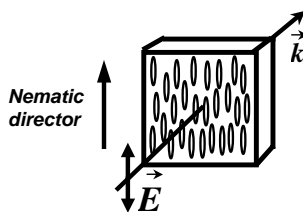
(b)

Fig. 1. (a) Experimental set up and (b) irradiation geometry of the planar nematic LC cell.

(a)

(b)

Fig. 2. (a) Molecular structure of the liquid crystal mixture E7 and (b) the dye "Oil Red O".

was used for filling the LC cells. E7 was supplied by EM-Industries; Oil Red O was supplied by Sigma-Aldrich.

Planar-aligned nematic LC-layers were prepared using buffing techniques on Nylon 6/6 alignment layers on Soda-Lime-glass plates of size 2.5 cm × 2.5 cm × 0.3 cm. Glass-bead-spacers mixed with an UV-epoxy provided cell thicknesses between 10 and 20 μm. Coating the substrates by Nylon 6/6, buffing, cell assembly, and filling the cells with LC were carried out in a clean room. UV-cured epoxy was used for sealing the cells.

It is very important that the dye possess dichroic properties. Cell transmittance at low incident intensities was $\sim 1\%$ for incident polarization parallel to the nematic director, and ~ 10–15% for the perpendicular polarization.

4. Results: Polarization-Dependent Spatial Patterns in the Beam Cross-Section

4.1. *Spatial pattern formation at low incident intensities* ($I \sim 1$–5 *MW/cm^2*)

The key characteristics of the effects we observed during repetitive illumination of the LC-cells by a focused laser beam for time spans of *several seconds* to *several minutes* are as follows:

- A *stable* far-field pattern of a "cross" appeared in the beam cross-section. The bright axes of the cross were oriented at 45° to the incident polarization (Fig. 3, left).
- A polarization component *perpendicular* to the nematic director appeared after the beam passed through the nematic layer.
- The *perpendicular* polarization component took on the far-field form of an optical four-leaf clover (Maltese-like cross); see Fig. 3, center.
- The incident, *parallel* polarization component evolved into the far-field pattern in the form of a ring with a bright spot inside (Fig. 3, right).
- *Stable* patterns existed for more than one hour of irradiation, but disappeared after switching the laser to a 5-Hz repetition rate.
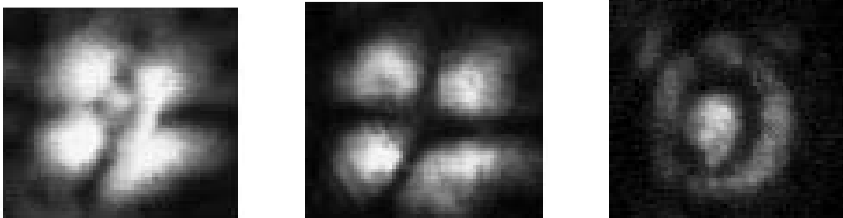

Fig. 3.   Far-field spatial patterns at low incident intensities: Left — no polarizer; center — perpendicular-polarization (induced) component; right — parallel (incident) polarization component.

4.2. *Spatial pattern formation at high incident intensities* ($I \sim 5{-}10$ *MW/cm^2*)

At higher incident intensities, high-definition patterns were observed only for the polarization component *parallel* to the nematic director. Figure 4 shows the beam cross-sections of two partially separated polarization components (using a Glan-prism) overlapping in the center. The left side of the image depicts *the parallel-polarization* component; the right side — *the perpendicular-polarization* component. The optical four-leaf-clover of the *perpendicular-polarization* component became smeared into a random speckle pattern with a bright spot in the center (see the right side of the image). At the same time, *the parallel-polarization* component developed a high-definition pattern that kaleidoscopically changed from pulse to pulse from rings (see left side of the Fig. 4 image) and stripes to multiple hexagons. A detailed description of this regime will be described elsewhere. The patterns disappeared after switching the laser to a 5-Hz repetition rate.

Figure 5 shows the near-field image of pattern similar to the far-field pattern of Fig. 4, left-side of the image. 500×-magnified, near-field image was recorded from the screen by the video camera. The sizes of various near-field spots were measured to be between 5 and 15 μm using both calibrated measurements in the near field and evaluation of the far-field images with angular dimensions between 0.04 and 0.13 rad.
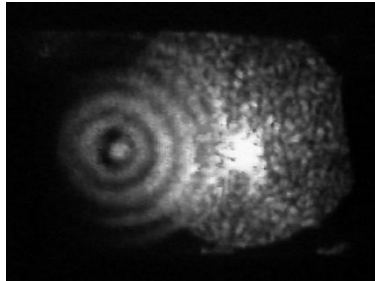

Fig. 4. Far-field spatial pattern at high incident intensity for the polarization component parallel to the director (left side of the image) and the perpendicular polarization component (right side of the image). A Glan prism was used to separate the two polarization states.
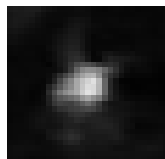

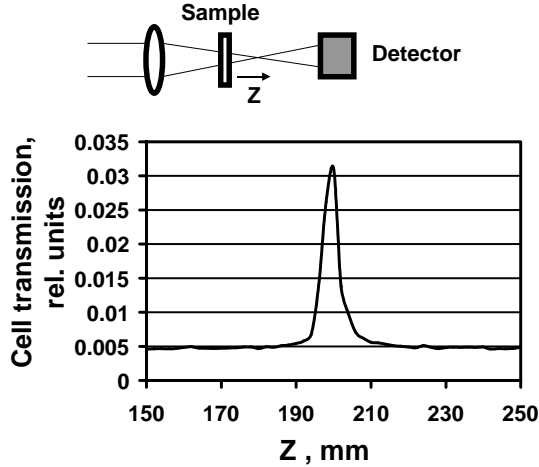Fig. 5. Near-field spatial pattern at high incident intensities.

Fig. 6.   *Z*-scan experimental set up (top) and *z*-scan curve of nonlinear change of transmission of a dye-doped planar-aligned liquid crystal cell at incident intensities below those for which pattern-formation occurs (bottom).

5. Results: *Z*-Scan Measurements of Nonlinear Transmission Enhancement of Dye-Doped Liquid Crystal Layers

To measure the changes in nonlinear transmission of dye-doped nematic liquid crystal layers, the open-aperture *Z*-scan method[8] was used. In this technique, a sample is scanned along the optical, *Z*-axis through the focus of a lens, while the far-field transmission is recorded as a function of sample position (Fig. 6, top). The nonlinear transmission changes are obtained by collecting light from the whole beam (open aperture *Z*-scan).

Figure 6, bottom shows a several-fold transmission enhancement upon irradiation of the dye-doped planar nematic LC-cell at an intensity below which pattern formation is observed.

6. The Mechanism of Laser-Induced Cumulative Birefringence Effects

Under the irradiation geometry (Fig. 1(b)) used in our experiments with the nematic director *parallel* to the incident polarization, no electric-field induced orientational phenomena should be observed to first order.[9] However, the birefringence effects reported here suggest the reorientation of LC molecules under laser irradiation. We believe that we can explain the appearance of the perpendicular polarization component by photochemical trans/cis conformational changes[10] of the azo-dye used in our experiments, as, for instance, was reported in Ref. 11 for other azo-dyes under nanosecond laser irradiation. The trans/cis photo-induced isomerization of the Oil Red O dye was also suggested in Ref. 12 for the explanation of their experiments on transient holograms in rigid dye solutions.

The mechanism of heat-flow[13,14] and/or flow-reorientational[14−18] birefringence caused by a spatial dependence of the temperature field is a likely explanation for the four-leaf-clover pattern at low incident intensities. At high incident intensities another mechanism is probably responsible for multiple ring pattern formation: the reorientation of a LC molecular director at the boundary of the isotropic liquid region/nematic LC as a result of heating of a nematic to the phase-transition temperature $T_c \sim 60°$C. The role of a *dichroic* azo-dye is to increase the contrast of the patterns to make them visible. We will consider next these two mechanisms separately.

6.1. *Low-incident-intensities birefringence mechanism*

Four-leaf-clover far-field patterns were observed earlier under *CW-irradiation*[19−22] of nematic[19,20] and smectic[21,22] LC layers with *homeotropic* alignment (LC-molecules were perpendicular to the substrate walls). Either order-electric effects[19,23] or thermomechanical effects[24] on the fluctuations of the director[20−22] were suggested as possible explanations of the reported phenomena. For our experiments, irradiation of the dye-doped *planar* nematic cell by *CW*-532-nm laser radiation did not show any four-leaf-clover patterns in the far-field.

Conditions closer to those of our experiments were reported in Ref. 14. A 10-μm-thickness *planar*-nematic *glassy* liquid crystal layer was irradiated by a single pulse of 20-ms duration. No far-field patterns were reported in this paper, but polarizing microscopy images showed a four-leaf-clover polarization pattern indicative of a frozen-in reorientation of the nematic molecules. Numerical modeling of the heat flow alignment in Ref. 14 showed that the reorientational phenomena in this case can be explained by stress-optical coupling similar to stress-induced birefringence, where the stress is caused by a locally inhomogeneous temperature field.

In distinction to nematic glassy liquid crystal[14] where no flow of material takes place, the additional mechanism of realignment in a nematic *liquid*, the so-called flow-alignment,[15−17] can contribute to the induced birefringence observed in our experiments. Under short-pulse irradiation of nematic LC layers, the flow is initiated by the large temperature and density changes.[9]

6.2. *High-incident-intensities-birefringence mechanism*

The maximum instantaneous temperature during a single pulse can be calculated as $T_{inst} = T_{room} + \varepsilon/\rho S h c_p$. At high incident intensities, for instance, at absorbed energy $\varepsilon \sim 25$ μJ, density $\rho = 1$ g/cm^3; cross-section $S = \pi(75 \, \mu\text{m})^2$; layer thickness $h = 10$ μm; heat capacity $c_p = 1.92$ J/gK, T_{inst} can reach 100°C which is far above the nematic/isotropic liquid phase transition temperature T_c.

Diffraction by an isotropic drop inside the nematic LC created by localized heating of the material above T_c was reported earlier for CW-irradiation in Refs. 25 and 26. Our results are the first manifestation of this effect for pulsed laser radiation.

Numerical modeling of heat-transfer in 10–20-μm thickness layers between glass substrates showed heat dissipation in a time interval of ~ 0.5 ms, which is much shorter than the time interval between two pulses in our experiments (100 ms). Similar numerical modeling has been undertaken in Ref. 27 for thin, 2-μm-thickness layers, where a ~ 10-μs heat dissipation time has been reported. Heat dissipation in much longer intervals ~ 100 ms was reported in Ref. 28 for *thick* ~ 100 μm layers. The additional mechanism of *heat isolation* should be taken into account in our experiments to explain the *cumulative* character of our observed phenomena.

7. Conclusion

The interaction of 20-ns-duration, 10-Hz-pulse-repetition-rate laser pulses at 532-nm wavelength with a planar-aligned, azo-dye-doped nematic liquid crystal layer has been studied for incident polarization *parallel* to the nematic director. New *cumulative* induced-birefringence effects were observed. They manifest themselves in (1) the appearance of a polarization component perpendicular to the nematic director and (2) two modes of spatial pattern formation with different patterns for parallel and perpendicular polarizations.

At low intensities (I ~ 1–5 MW/cm^2), far-field spatial birefringence patterns are different for each polarization, e.g. a four-leaf-clover was observed in the laser-induced (*perpendicular* to the nematic director) polarization component. At the same time, a central bright spot with a ring appeared in the parallel polarization component. This birefringence effect can be explained by laser-induced heat flow and/or flow of nematic liquid, leading to molecular reorientation of LC and dichroic dye molecules. Accumulation of molecular reorientation from pulse to pulse gives rise to stable pattern formation in the laser beam.

At high-intensities (I ~ 5–10 MW/cm^2), high-definition patterns were observed only for the polarization component *parallel* to the nematic director. Diffraction of laser light by the isotropic liquid region as a result of a nematic/isotropic phase nucleation can account for the concentric ring structure of the observed far-field patterns. Phase separation of the dye molecules from the LC host can also contribute to amplitude and phase inhomogeneity in the laser beam.

One of the authors (Svetlana G. Lukishova) wrote her Ph.D Thesis under the supervision of Prof. Alexander Mikhailovich Prokhorov at the Oscillations Laboratory of the P. N. Lebedev Physical Institute (later the General Physics Institute) of the Russian Academy of Sciences (Moscow), where A. M. Prokhorov and N. G. Basov had created their ammonia molecular generator. At one of the Anniversaries of this Laboratory, Alexander Mikhailovich emphasized that the style of the Laboratory always was to combine Science with Merriment and Humor. This certainly also reflected his own style in life. This combination of his bright mind with humor, remarkable scientific intuition, enormous knowledge (he was an Editor-in-Chief of the many-volume Great Russian Encyclopedia) to understand all papers of his colleagues had written in different scientific fields, and genius of leadership made him unique. His energy permitted him to be the Director of the General Physics Institute, the Academician-Secretary of the Academy of Science Headquarters (Presidium) who defined the scientific and budget policies of the Soviet/Russian Department of General Physics and Astronomy. In addition, he was Chairman of Divisions of two Soviet/Russian competitive educational institutes in the field of physics and mathematics, namely the Moscow Institute of Physics and Technology (FizTech) and the Physics Department at Moscow State University. It is important to add that in spite of his busy schedule, A. M. Prokhorov never hesitated to use his high administrative positions in the Soviet/Russian society to help other people in difficult situations.

Among more than 1500 papers written by A. M. Prokhorov both solely and with co-authors in various areas of Quantum Electronics, from radiospectroscopy and masers to laser physics, applications and interaction of laser radiation with matter, several well-known papers were devoted to various effects of high-power laser interaction with absorbing liquid media, for instance, Refs. 29–31. Here we present a paper on the interaction of repetitive-pulse laser radiation with dye-doped liquid crystal layers. To follow the style of A. M. Prokhorov in combining research with real device fabrication, we hope that this research will help us in understanding the limits in a photonic device we are working with right now: a dye-doped liquid crystal single-photon source[32] for quantum information and communication.

References

1. C. Umeton, G. Cipparrone and F. Simoni, *Opt. Quantum Electron.* **18** (5), 312 (1986).
2. S. G. Lukishova, *J. Nonlin. Opt. Phys. Mat.* **9** (3), 365 (2000).
3. L. S. Goldberg and J. M. Schnur, *U.S. Patent*, No. 3,771,065 (1973).
4. I. P. Il'chishin, E. A. Tikhonov, V. G. Tishchenko and M. T. Shpak, *JETP Lett.* **32**, 24 (1980).
5. V. P. Kopp, B. Fan, H. K. M. Vithana and A. Z. Genack, *Opt. Lett.* **23**, 1707 (1998).
6. B. Taheri and P. Palffy-Muhoray, *ALCOM Update* **9** (1), 7 (1999).
7. *Solid State Sources for Single Photons*, www.iota.u-psud.fr/~S4P/.
8. M. Sheik-Bahae, A. A. Said, T.-H. Wei, D. J. Hagan and E. W. Van Stryland, *IEEE J. Quantum Electron.* **26**, 760 (1990).

9. I.-C. Khoo, *Liquid Crystals, Physical Properties and Nonlinear Optical Phenomena* (John Wiley & Sons, New York, 1995).

10. L. F. Fieser and M. Fieser, *Advanced Organic Chemistry*, p. 691 (Reinhold Publ., New York, 1963).

11. S. Serak, A. Kovalev, A. Agashkov, H. F. Gleeson, S. J. Watson, V. Reshetnyak and O. Yaroshchuk, *Opt. Commun.* **187**, 235 (2001).

12. L. Nikolova, K. Stoyanova, T. Todorov and V. Taranenko, *Opt. Commun.* **64**(1), 75 (1987).

13. D. R. Baals and S. Hess, *Z. Naturforsch.* **40a**, 3 (1985).

14. R. Elscher, R. Macdonald, H. J. Eichler, S. Hess and A. M. Sonnet, *Phys. Rev.* **E60**, 1792 (1999).

15. I. C. Khoo, R. G. Lindquist, R. R. Michael, R. J. Mansfield and P. LoPresti, *J. Appl. Phys.* **69**, 3853 (1991).

16. H. J. Eichler and R. Macdonald, *Phys. Rev. Lett.* **67**, 2666 (1991).

17. R. S. Akopyan, B. Ya. Zel'dovich and N. V. Tabiryan, *Tech. Phys.* **38**(6), 493 (1994).

18. C. Glorieux, K. A. Nelson, G. Hinze and M. D. Fayer, *J. Chem. Phys.* **116**, 3384 (2002).

19. G. Hu and P. Palffy-Muhoray, *Mol. Cryst. Liq. Cryst.* **304**, 447 (1997).

20. M. I. Barnik, A. S. Zolot'ko and V. F. Kitaeva, *JETP* **84**, 1122 (1997).

21. A. S. Zolot'ko, V. F. Kitaeva and D. B. Terskov, *Sov. Phys. JETP* **74**, 974 (1992).

22. M. I. Barnik, V. F. Kitaeva, V. G. Rumyantsev and A. S. Zolot'ko, *Mol. Cryst. Liq. Cryst.* **299**, 91 (1997).

23. G. Barbero, I. Dozov, J. F. Palierne and G. Durand, *Phys. Rev. Lett.* **56**, 2056 (1986).

24. R. S. Akopyan and B. Ya. Zel'dovich, *Sov. Phys. JETP* **60**, 953 (1984).

25. V. Volterra and E. Wiener-Avnear, *Appl. Phys.* **6**, 257 (1975).

26. F. Bloisi, L. Vicari, F. Simoni, G. Cipparrone and C. Umeton, *J. Opt. Soc. Am.* **B5**, 2462 (1988).

27. D. Grebe and R. Macdonald, *J. Phys.* **D27**, 567 (1994).

28. H. Hsiung, L. P. Shi and Y. R. Shen, *Phys. Rev.* **A30**, 1453 (1984).

29. G. A. Askar'yan, A. M. Prokhorov, G. F. Chanturiya and G. P. Shipulo, *Sov. Phys. JETP* **17**, 1463 (1963).

30. F. V. Bunkin, V. I. Konov, A. M. Prokhorov, V. V. Savransky and V. B. Fedorov, *Sov. Phys. JETP* **40**, 1036 (1974).

31. K. L. Vodop'yanov, L. A. Kulevskii, P. P. Pashinin and A. M. Prokhorov, *Sov. Phys. JETP* **55**, 1049 (1982).

32. S. G. Lukishova, A. W. Schmid, A. J. McNamara, R. W. Boyd and C. R. Stroud, *Opt. Soc. Am. Tech. Dig. Ser. QELS'03* (2003).